Dalton Transactions

Insight into the nature of M-C bonding in the lanthanide/actinide-biscarbene complexes: A theoretical perspective

Journal:	*Dalton Transactions*
Manuscript ID	DT-ART-07-2018-002702.R1
Article Type:	Paper
Date Submitted by the Author:	12-Aug-2018

Complete List of Authors:	Wu, Qunyan; Institute of High Energy Physics Chinese Academy of Sciences, Cheng, Zhongping; Institute of High Energy Physics, Laboratory of Nuclear Energy Chemistry Lan, Jianhui; Institute of High Energy Physics, Chinese Academy of Sciences, Laboratory of Nuclear Energy Chemistry Wang, Congzhi; Institute of High Energy Physics Chinese Academy of Sciences Chai, Zhifang; Institute of high energy physics, Laboratory of Nuclear Energy Chemistry Gibson, John; Lawrence Berkeley National Laboratory, Chemical Sciences Division Shi, Weiqun; Institute of High Energy Physics, Laboratory of Nuclear Energy Chemistry;

Journal Name

ARTICLE

Insight into the nature of M-C bonding in the lanthanide/actinide-biscarbene complexes: A theoretical perspective

Received 00th January 20xx,
Accepted 00th January 20xx

DOI: 10.1039/x0xx00000x

www.rsc.org/

Qun-Yan Wu,[a] Zhong-Ping Cheng,[a] Jian-Hui Lan,[a] Cong-Zhi Wang,[a] Zhi-Fang Chai,[ab] John K. Gibson,[c] and Wei-Qun Shi*[a]

We have investigated M-C bonds in lanthanide and actinide complexes ML_2 (M=Ce, Th, U, Np and Pu; L=C($PPh_2NMes)_2$) using scalar-relativistic theory. The M-C bonds possess typical σ and π bonding character, except for the nearly π-only Th-C bonds. The metal valence electrons significantly reside in the valence d and f orbitals for CeL_2, UL_2, NpL_2 and PuL_2, while for ThL_2 most electron population is in 6d orbitals. The contribution of 6d orbitals to the An-C bonds decreases and that of 5f orbitals increases across the actinide series. QTAIM (quantum theory of atoms in molecules) and NBO (natural bond orbital) analyses confirm that the M-C bonds possess significant covalent character. This work provides insights into the contributions of d and f valence orbitals to M-C bonding. And inclusion of Np and Pu in this evaluation extends understanding to later actinides.

Introduction

Transition metal carbenes having M-C bonds have received wide attention in the past decades due to extensive applications in the fields of catalysis[1-3] and organometallic chemistry.[4, 5] In contrast, the chemistry of f-block metal carbon multiple bonds is underdeveloped. Cramer and coworkers reported the first uranium-carbene complex, [(η^5-$C_5H_5)_3$U=CHP($CH_3)_2$(C_6H_5)], in 1981.[6] During the past two decades, several f-block metal carbene complexes have been reported.[7-25] For instance, Cavell and coworkers provided the first structure of a samarium(III) carbene complex in 2000.[7] Le Floch et al. synthesized homoleptic Sm(III) and Tm(III) biscarbene complexes,[8, 9] and subsequently employed the same carbene ligand to obtain a uranium complex with a U=C double bond.[10] Liddle and coworkers synthesized the first homoleptic uranium(IV) biscarbene complex, [U(C($PPh_2NMes)_2)_2$] (Mes = 2,4,6-$Me_3C_6H_2$) (Scheme 1), with two formal U=C double bonds.[11] This same group recently prepared the cerium(IV) carbene complex [Ce(BIPM^{TMS})(ODipp)$_2$] with σ- and π-bonding character,[17] and three new metal biscarbene complexes [M(BIPM^{TMS})$_2$] (M=Ce, Th, U) bearing M=C double bonds.[23] Zi and coworkers prepared and characterized the first thorium(IV) poly-carbene complexes with polarized Th=C bonds.[12] Several uranium complexes with U=C double bonds have been synthesized using formally dianionic ligands.[26, 27] Andrews and coworkers reported complexes such as HC≡UX_3 and H_2C=UX_2 (X=H, F, Cl, Br) in cryogenic noble gas matrices.[28-30]

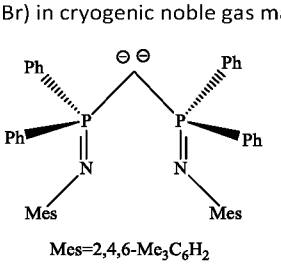

Mes=2,4,6-$Me_3C_6H_2$

L

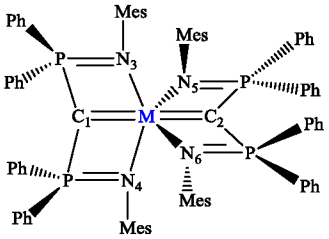

ML_2 (M=Ce, Th, U, Np, Pu)

Although the nature of lanthanide (Ln)- and actinide (An)-ligand multiple bonds have been investigated both experimentally and theoretically,[31-35] understanding the nature of actinide multiple bonds remains particularly challenging due to the unique and complex electronic structures of the actinides. Theoretical studies have provided insights into participation of 5f/6d valence orbitals in chemical bonding for actinide complexes bearing actinide multiple bonds, such as actinide-carbon multiple bonds.[18, 23, 36-39] It is clearly desirable to better understand the nature of bonding in Ln(IV)- and An(IV)-biscarbene complexes, including comparisons between Ln=C and An=C bonds. Extending these evaluations beyond U in the actinide series, specifically to Np and Pu, is necessary to elucidate the changing role of the 5f electrons across the series.

[a] Laboratory of Nuclear Energy Chemistry, Institute of High Energy Physics, Chinese Academy of Sciences, Beijing, 100049, China. E-mail: shiwq@ihep.ac.cn
[b] School of Radiological and Interdisciplinary Sciences (RAD-X), and Collaborative Innovation Center of Radiation Medicine of Jiangsu Higher Education Institutions, Soochow University, Suzhou 215123, China
[c] Chemical Sciences Division, Lawrence Berkeley National Laboratory, Berkeley, California, 94720, USA

Electronic Supplementary Information (ESI) available: Structures of the complexes ML_2 (M=Ce, Th, U, Np, Pu); LUMO and SOMOs of ML_2 (M=U, Np, Pu); natural bond orbitals between metal atom and carbon atom of carbene ligands; ELF of (M=Ce, Th, Np, Pu); calculated U-C and U-N bond distances in complex UL_2 in toluene solution using BP86, B3LYP, M06 and M06L functionals with 6-31G(d) basis set; calculated compositions (%) of Kohn Sham frontier MOs and NBOs for the five ML_2. See DOI: 10.1039/x0xx00000x

Based on the reported structure of the homoleptic uranium(IV) biscarbene complex [UL_2, L=C($PPh_2NMes)_2$],[11] we selected it and its counterparts with M=Ce, Th, Np and Pu shown in Scheme 1, to evaluate the electronic structures and the bonding of Ln(IV)- and An(IV)-biscarbenes with a goal of furthering comprehension of the nature of bonding in f-block element carbene complexes.

Computational Details

The structure optimizations of the metal-biscarbene complexes were carried out using density functional theory (DFT) with the Gaussian 09 program.[40] To examine the reliability of various methods, the structure of the UL_2 complex obtained from its crystal structure[11] was optimized using the generalized gradient approximation (GGA) BP86,[41] hybrid GGA B3LYP,[42, 43] meta GGA M06 and M06L[44] functionals. Because the UL_2 complex was crystallized in toluene solution, the optimization was considered in the same solvent using CPCM (conductor-like polarizable continuum model) with the Klamt atomic radii.[45, 46] Bond distances of UL_2 obtained with BP86 functional are in the best accord with available crystal data, as discussed below. The structures of the analogous complexes with U replaced by Ce, Th, Np and Pu were optimized using the BP86 functional. The scalar-relativistic small-core pseudopotential ECP60MWB[47, 48] for the 5f-block metals (Th, U, Np and Pu) and ECP28MWB[49, 50] for Ce, as well as the corresponding segmented valence basis sets were applied;[47, 48, 50] the 6-31G(d) basis set was used for C, H, N and P. The singlet CeL_2 and ThL_2, triplet UL_2, quartet NpL_2, and quintet PuL_2 are the ground state configurations based on the total electronic energies in Table S1 of electronic supplementary information (ESI), in accord with the highest spin state of actinide ions typically being the ground state for such actinide complexes.[51, 52] Harmonic vibrational frequencies of the optimized structures of the ML_2 complexes are all positive values at the same level of theory. In addition, the spin contaminations of three UL_2, NpL_2 and PuL_2 complexes are neglected because of <S2> values close to the ideal values of S(S + 1).

Natural population analyses were performed using the NBO (natural bond orbital) method with NBO program as implemented in Gaussian 09 program. NBO calculations were carried out using BP86 with a higher quality basis set, cc-pVTZ, at the corresponding BP86/ECP/6-31G(d) optimized structures. The extended transition state (ETS) method with the natural orbitals for the chemical valence (NOCV) theory[53] was performed to further reveal the bonding nature using the Amsterdam density functional (ADF 2013.01) package.[54] The BP86 method and the Slater type orbital (STO) basis set with the quality of triple-ζ plus polarization (TZP)[55] was employed without frozen core. Scalar relativistic (SR) effects were taken into account using the zero-order regular approximation (ZORA) approach.[56] The topological analysis based on the wave functions obtained at the BP86/ECP/cc-pVTZ level of theory was carried out using the quantum theory of atoms in molecules (QTAIM)[57] with the Multiwfn program.[58]

Results and discussion

Structures of the ML_2 complexes.

Various methods have been employed to study geometric and electronic structures, and related properties of actinide complexes.[52, 59-61] To test the reliability of different functionals for predicting geometrical parameters for the ML_2 complexes, four functionals, BP86, B3LYP, M06 and M06L, were adopted to optimize the structure of the UL_2 complex, for which experimental crystal structure data are available.[11] The U-C and U-N bond distances obtained in toluene solution using four functionals with 6-31G(d) basis set are presented in Table S2. It is apparent that the average relative errors in bond distances with BP86 are the smallest among the four functionals. In particular, the key U-C_1 and U-C_2 bonds distances using the BP86 functional are very close to the experimental values, with relative differences of < 0.8% when the maximum uncertainties in the experimental values are considered. The structure of UL_2 is also optimized using larger basis set 6-311G(d) with BP86 functional, the average relative errors are similar to those with 6-31G(d) basis set (Table S2). Hence, the structures of the UL_2 analogues, CeL_2, ThL_2, NpL_2 and PuL_2, were optimized at the BP86/ECP/6-31G(d) level of theory.

In Table 1 are given the selected bond distances and angles of the five ML_2 complexes (Figure S1) optimized at the BP86/ECP/6-31G(d) level of theory in toluene solution. As the geometrical parameters indicate, the five ML_2 complexes have similar structures consisting of two quasi-planar four-membered CMNP rings in each ligand as shown in Figure S2 with the simplified structure of ML_2. These two CMNP rings in the same carbene ligand construct 'open book'[62] conformations with PCP angles of about 135°, and the two carbene ligands are almost orthogonal to each other with angles of 85.21-87.15° for the five ML_2 complexes. The C_1MC_2 angles are about 145-148°, deviated significantly from linearity, which leads to a distorted octahedral structures. Despite the similar structures there are clear differences between the M-C bond distances in the five complexes. The An-C (An=Th, U, Np, Pu) bond distances gradually decreases across the actinide series, which is in accord with the trend of ionic radii for An^{IV}: Th^{IV}=0.94 Å, U^{IV}=0.89 Å, Np^{IV}=0.87 Å, Pu^{IV}=0.86 Å.[63] However, the calculated U-C and Ce-C bond distances do not correlate with the corresponding ionic radii (Ce^{IV}=0.87 Å).[63] The calculated Ce-C bond distance in the CeL_2 complex is 2.441 Å, which is comparable to that in the complex [Ce($BIPM^{TMS}$)(ODipp)$_2$] (2.441(5) Å) with both Ce-C σ and π bonding according to NBO analysis.[17] These Ce-C bond distances are only slightly longer than those for [Ce($BIPM^{TMS}$)$_2$] (2.385(2) and 2.399(3) Å), which exhibits Ce-C multiple bond character,[23] suggesting that the Ce-C bonds in CeL_2 complex also possess multiple bond character. The Th-C bond distance (2.527 Å) is the longest among the five complexes, and is ~0.01 Å longer than in [Th($BIPM^{TMS}$)$_2$] (2.514(3) and 2.516(3) Å),[23] and is also somewhat longer than that in complexes [Th($BIPM^{TMS}$)(ODipp)$_2$] (2.508(5) Å)[17] and [Th($BIPM^{TMS}$)(η^5-C_5H_5)$_2$] (2.436(4) Å).[64] The calculated U-C bond distance is

2.432 Å in the UL_2 complex, which is comparable to the corresponding experimental distances from the crystal structure (2.427 (8) and 2.448 (9) Å).[11] This distance is longer than in $[U(BIPM^{TMS})_2]$ (2.410(6) and 2.421(6) Å)[23] and $[U(BIPM^{TMS})(ODipp)_2]$ (2.414(3) Å).[17] Complex PuL_2 adopts the shortest M-C bond distance, 2.397 Å, among the five ML_2 complexes. It is also notable that there is 0.05 Å gap between the longest M-N bonds for Ce-N (2.546 Å) and the shortest such bonds for U-N (2.496 Å).

Table 1 M-C and M-N bond distances (Å) and selected bond angles (degrees) in the ML_2 complexes at the BP86/ECP/6-31G(d) level of theory.

complexes	CeL_2	ThL_2	UL_2	NpL_2	PuL_2
M-C	2.441	2.527	2.432	2.412	2.397
M-N	2.546	2.532	2.496	2.511	2.540
PC_1P	135.89	134.75	135.70	135.57	135.82
C_1MC_2	148.05	145.69	144.85	145.54	146.85
N_3MN_4	113.58	112.13	115.30	114.71	114.09
$N_4MC_1N_3$	137.40	136.57	139.00	138.58	138.12
D_L[a]	87.15	85.21	86.47	86.38	85.33

[a] D_L denotes the angle between two quasi-planar four-membered CMNP rings in each carbene ligand.

Molecular orbitals.

GGA BP86, PBE and hybrid B3LYP, PBE0 were used to evaluate the ground state electronic structures of three open shell structures (UL_2, NpL_2 and PuL_2). The composition of the metal atom for the singly occupied alpha-spin MOs (SOMOs) as presented in Table S3 indicates that the electron density obtained by GGA is more localized on the metal atom than that by the hybrid functionals. Therefore, the GGA BP86 was selected to describe the ground state electronic structures studied here, although some studies reported that hybrid functions can better predict the ground state electronic structure of the actinide complexes.[65] SOMOs of the three ML_2 (M=U, Np, Pu) complexes obtained with BP86 functional are presented in Figure S3, showing their electron densities predominantly localized on the metal atoms (essentially pure 5f character) according to the compositions of the MOs in Table S4. This result indicates that the electronic configurations of UL_2, NpL_2 and PuL_2 are essentially $5f^2$, $5f^3$ and $5f^4$, respectively. The lowest unoccupied MO (LUMO) of the five ML_2 complexes (Figure S4), indicating that the electron density is also mainly localized on the metal atom, except for ThL_2 complex. This probably be one reason why Th-C bonds have different bonding characteristics compared to other M-C (M=Ce, U, Np, Pu) bonds as discussed below. Three highest double-occupied MOs (HOMOs) of the five ML_2 complexes are displayed in Figure 1, which clearly display σ and π bonding interactions between metal centers and C atoms based on the diagrams and the corresponding compositions (Table S4) of the MOs. Taking the CeL_2 complex as an example, the HOMO including 17.2% Ce and 19.8/20.4% C_1/C_2 character reveals a Ce-C σ bonding interaction. The composition of HOMO-1 is 5.8% Ce and 20.1/23.6% C_1/C_2 character, indicating Ce-C π bonding interactions. HOMO-2 exhibits high 9.3% Ce and 20.5/14.7% C_1/C_2 contributions. Notably, the contributions of all five M are smaller than those of C_1/C_2 for HOMO, HOMO-1 and HOMO-2, indicating polarized M-C bonds. Moreover, the metal contribution to the doubly occupied MOs is greatest in PuL_2 among the five complexes. Energy levels of LUMOs, SOMOs and HOMOs for the five ML_2 complexes are also presented in Figure 2. It clearly shows that the energies of the HOMO gradually decrease across the actinide series from Th, U, Np to Pu, which suggests better atomic orbital energy matching between the actinides and carbene ligands. And the trend of LUMO, HOMO-1, HOMO-2 and three SOMOs appears similar result, respectively. The HOMO of CeL_2 has almost the same energy as that of UL_2, in accord with the similar structural properties of CeL_2 and UL_2.

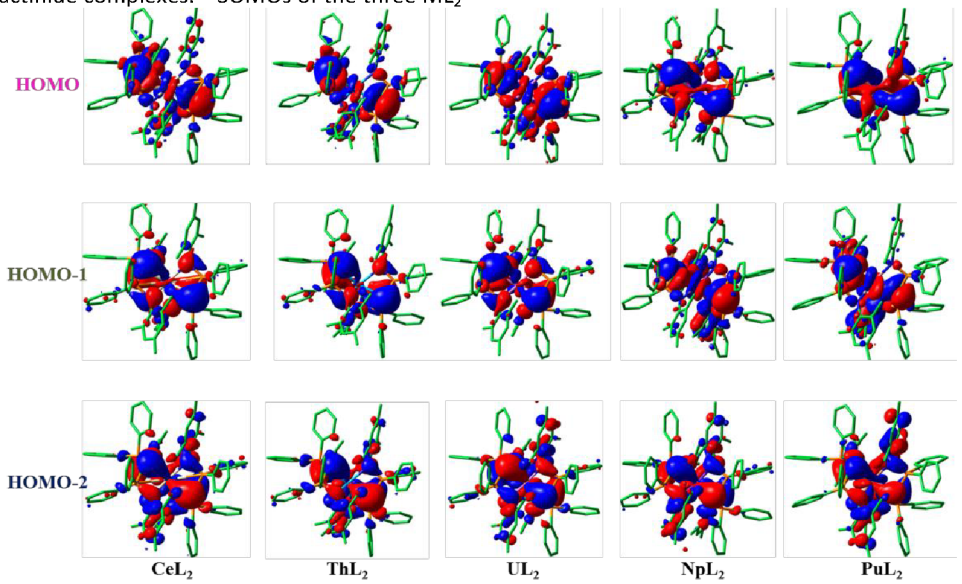

Fig. 1 Three highest double-occupied MO (HOMO) diagrams of the five ML_2 (M=Ce, Th, U, Np, Pu) complexes in toluene solution.

Journal Name

ARTICLE

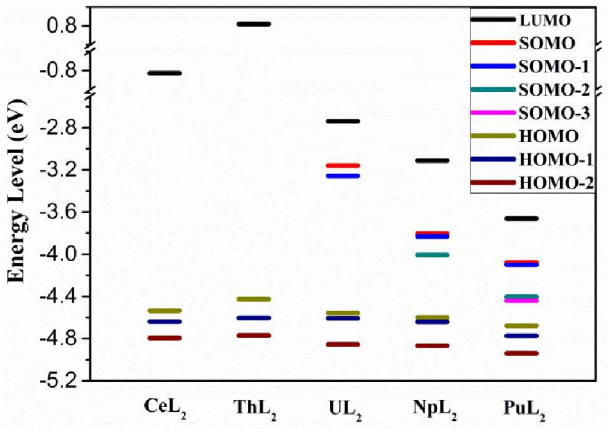

Fig. 2 Energy levels of LUMOs, SOMOs and HOMOs for the five ML_2 complexes in toluene solution at the BP86/ECP/cc-pVTZ level of theory.

NBO analysis

We performed NBO analysis with the BP86 method to further elucidate the nature of bonding in the ML_2 complexes. The valence electron populations of the metals in ML_2 are given in Table 2. The valence electrons of Ce in CeL_2 mainly reside in the 4f and 5d orbitals, while for Th in ThL_2 the occupation is primarily in 6d, with little in 5f orbitals; this disparity likely reflects the different bonding nature in the Ce and Th complexes, as discussed below. The U, Np and Pu valence electrons reside primarily in 5f orbitals, with occupations of 3.18, 4.29 and 5.30, respectively, while only 1.24 (U), 1.15 (Np) and 1.07 (Pu) electrons are in 6d orbitals. The occupation of 7p orbitals is nearly the same (0.21) for the four AnL_2 complexes, which is somewhat less than the 6p orbitals occupation (0.28) in CeL_2. Mulliken charges on the metal atoms are 1.03-1.49 for the ML_2 complexes (Table 2), indicating significant formal charge transfer from carbene ligands to the metal atoms. The values of Δq in Table 2 are defined as the charge transfer to a formally +4 metal ion, to result in the substantially lower actual positive charges, $q<<4$, on the metals in the ML_2 complexes. This formal charge transfer can be employed to evaluate the magnitude of the bonding interaction between the actinides and carbene ligands, resulting in the following ordering: PuL_2 (greatest charge transfer) > NpL_2 > UL_2 > ThL_2 (least charge transfer); this order is in agreement with the HOMO energy analysis. And the values of Mulliken spin density also indicate the same trend. In addition, Mayer bond order (MBO)[66] for the M-C bonds are also presented in Table 2. The value of Th-C MBO is clearly the smallest among the five M-C bonds, indicating relatively weak Th-C bonding interaction.

Table 2 Population of valence electron, Mulliken spin density (Ms), Mulliken charge (q) of metal atom and the formal charge transfer from the ligand to the tetravalent metal ($\Delta q \equiv +4.00 - q$) as well as the M-C Mayer bond order (MBO) for the ML_2 complexes at the BP86/ECP/cc-pVTZ level of theory.

ML_2	Population of valence electron				Ms	q	Δq	MBO
CeL_2	6s(0.07)	6p(0.28)	5d(1.22)	4f(1.15)	0	1.03	2.97	0.904
ThL_2	7s(0.07)	7p(0.21)	6d(1.20)	5f(0.15)	0	1.49	2.51	0.724
UL_2	7s(0.07)	7p(0.21)	6d(1.24)	5f(3.18)	2.26	1.38	2.62	0.820
NpL_2	7s(0.08)	7p(0.21)	6d(1.15)	5f(4.29)	3.44	1.25	2.75	0.857
PuL_2	7s(0.08)	7p(0.22)	6d(1.07)	5f(5.30)	4.70	1.18	2.82	0.872

Table 3 Calculated NBO compositions of the M-C bonds at the BP86/ECP/cc-pVTZ level of theory.

M-C	type	M%	C%	M AOs (%)	C AOs (%)
Ce-C	σ	19.08	80.92	6p(6.34)5d(48.09)4f(44.99)	2s(23.10)2p(76.54)
	π	14.24	85.76	6p(3.35)5d(44.24)4f(51.42)	2s(1.52)2p(98.15)
Th-C	π	9.86	90.14	7p(3.17)6d(48.66)5f(47.42)	2p(99.44)
U-C	σ	19.07	80.93	6d(41.35)5f(57.13)	2s(26.48)2p(73.08)
	π	16.53	83.47	7p(1.73)6d(45.50)5f(52.12)	2p(99.03)
Np-C	σ	20.87	79.13	6d(38.77)5f(60.25)	2s(23.41)2p(76.19)
	π	19.59	80.41	7p(1.60)6d(44.00)5f(53.65)	2p(98.04)
Pu-C	σ	26.05	73.95	6d(41.84)5f(57.36)	2s(15.86)2p(83.88)
	π	21.22	78.78	7p(1.50)6d(35.72)5f(61.66)	2s(6.75)2p(92.83)

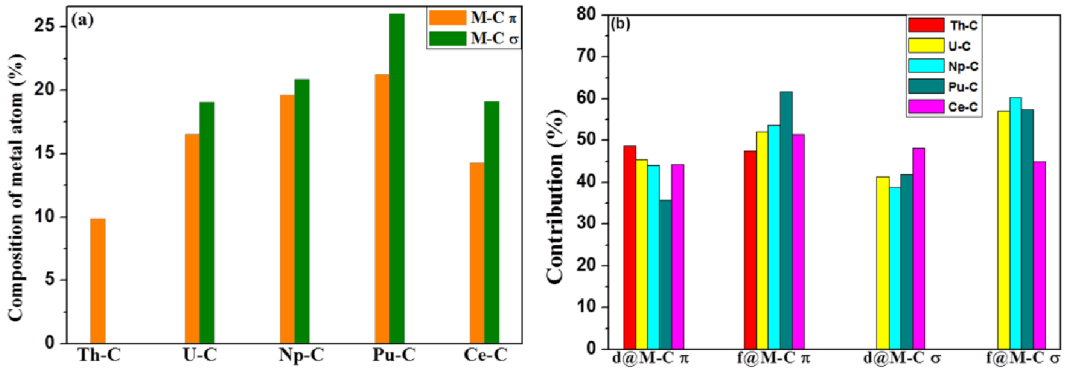

Fig. 3 Composition of metal atom (a) and the contribution of metal 4/5f and 5/6d orbitals to M-C π and σ bonds (b).

To obtain further insights about the M-C bonds in the ML_2, we performed the localized NBO analysis. The natural localized molecular orbitals (Figure S5) show distinct M=C σ and π bonding in the complexes CeL_2, UL_2, NpL_2 and PuL_2, but only Th-C π bonding in ThL_2 with the contribution of σ bonding below the default NBO cut-off value of 5%. In Table 3 are given the compositions of natural bond orbitals and the contributions of each atomic orbital of metal and carbon atom to the M-C bonds in ML_2. The carbon contribution (over 74%) to both the M-C σ and π bond is much larger than that of the metal atom, an effect that is particularly pronounced for the Th-C bonds. This analysis indicates partly polarized M-C bonds, in accord with recent reports.[12, 23, 37] Figure 3(a) clearly shows that the contribution of the actinide atom to both the An-C σ and π bonding increases with increasing actinide atomic number probably due to the better energy matching and overlap between the actinide atom and carbene ligands. The metal contribution is almost the same for the Ce-C and U-C bonds, which suggests similar character of these bonds. The metal contribution to the M-C σ bond is somewhat larger than to the M-C π bond. The (n-2)f and (n-1)d orbitals of the metals provide the dominant contributions to the σ and π bonding, with minor metal np orbital contribution (Table 3). As is apparent in Figure 3(b), the contribution of the An 6d and 5f orbitals is almost the same for the U-C and Pu-C σ bonds, while for the An-C π bonds, the 6d orbital contribution decreases and that of the 5f orbital increases from Th-C to Pu-C. The contribution of Ce 4f and 5d to the Ce-C π bonds, 51.42% and 44.24%, respectively, is similar to the respective contributions of U 5f and 6d orbitals to the U-C π bonds. Again, a remarkable similarity between bonding in the CeL_2 and UL_2 complexes is apparent.

Topological analysis.

QTAIM analysis based on the electronic density provides many properties regarding chemical bonding,[57] especially in the area of f-element bond characterization.[38, 67-74] QTAIM analyses were performed on the basis of the wave function obtained at the BP86/ECP/cc-pVTZ of theory to assess the covalency of the M-C bonds in ML_2 complexes. In general, an electron density (ρ(r)) at the bond critical point (BCP) greater than 0.20 au, together with a negative Laplacian ($\nabla^2\rho$(r)), denotes a covalent bond, while ρ(r) less than 0.10 au with a positive $\nabla^2\rho$(r) indicates an ionic bond. Furthermore, the total energy density (H(r)), the sum of the kinetic energy density (G(r)) and the potential energy density (V(r)), can be employed to evaluate the degree of bond covalency.[75] In principle, a negative H(r) value indicates a covalent bonding interaction with significant sharing of electrons. Strongly polar bonds are characterized by low values of ρ(r), which indicates local charge depletion. Another covalency parameter is $-V(r)/G(r)$: $-V(r)/G(r) > 2$ suggests a typical covalent bond, $-V(r)/G(r) < 1$ describes a classical ionic interaction, and $1 < -V(r)/G(r) < 2$ denotes intermediate bonding character with significant covalency. Table 4 collects the calculated QTAIM parameters at the M-C BCPs in the ML_2 complexes. The values of ρ(r) at the M-C BCPs are less than 0.1 due to the nature of the polarized bonds. The negative H(r) values suggest that the M-C bonds possess some covalent character and the Th-C bonds have the smallest covalent character based on the H(r) values, in agreement with the Mulliken charge analysis. The combined NBO and QTAIM analyses reveal that greater participation of the f orbitals in bonding can result in enhanced covalency. The ratio $-V(r)/G(r)$ for all M-C bonds close to 1.5 indicates that the M-C bonds have a significant degree of covalent character. In addition, ELF (electron localization functions) =1 suggests complete electron localization, while ELF=0 denotes complete delocalization.[76-78] Diagrams of ELFs at the M-C BCPs (Figures 4 and S6) also support the conclusion that the M-C bonds exhibit a significant degree of covalent character.

Table 4 Calculated QTAIM parameters at the M-C BCPs in the ML_2 complexes.

	ρ(r)	$\nabla^2\rho$(r)	-H(r)	G(r)	-V(r)	-V(r)/G(r)
Ce-C	0.0745	0.0815	0.0212	0.0212	0.0627	1.510
Th-C	0.0699	0.0795	0.0196	0.0196	0.0592	1.497
U-C	0.0804	0.1013	0.0239	0.0239	0.0730	1.485
Np-C	0.0818	0.1102	0.0242	0.0242	0.0760	1.468
Pu-C	0.0824	0.1120	0.0246	0.0246	0.0772	1.468

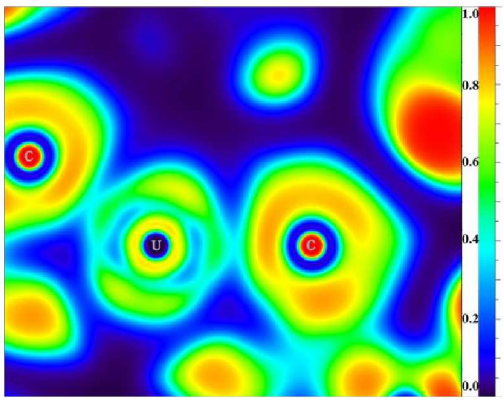

Fig. 4 Two dimensional ELF contour of the CMC plane containing the two M-C bonds for the UL_2 complex.

NOCV analyses.

To further reveal the covalent contribution to bonding between the metal and carbene ligands, the ETS-NOCV analysis was carried out based on the fragment calculations at the BP86/SR-ZORA/TZP level of theory using the ADF program. The three NOCVs with the largest contribution to the orbital interaction energy for each ML_2 are presented in Figure 5. It is notable that the contribution of the orbital interactions to the M-C bond is larger than that to M-N bond for the five ML_2 based on the NOCV orbital interaction energies. Moreover, the Th-C bonds appear to have less covalent character compared to those of the other M-C bonds (M=Ce, U, Np, Pu), which is accord with the above assessments.

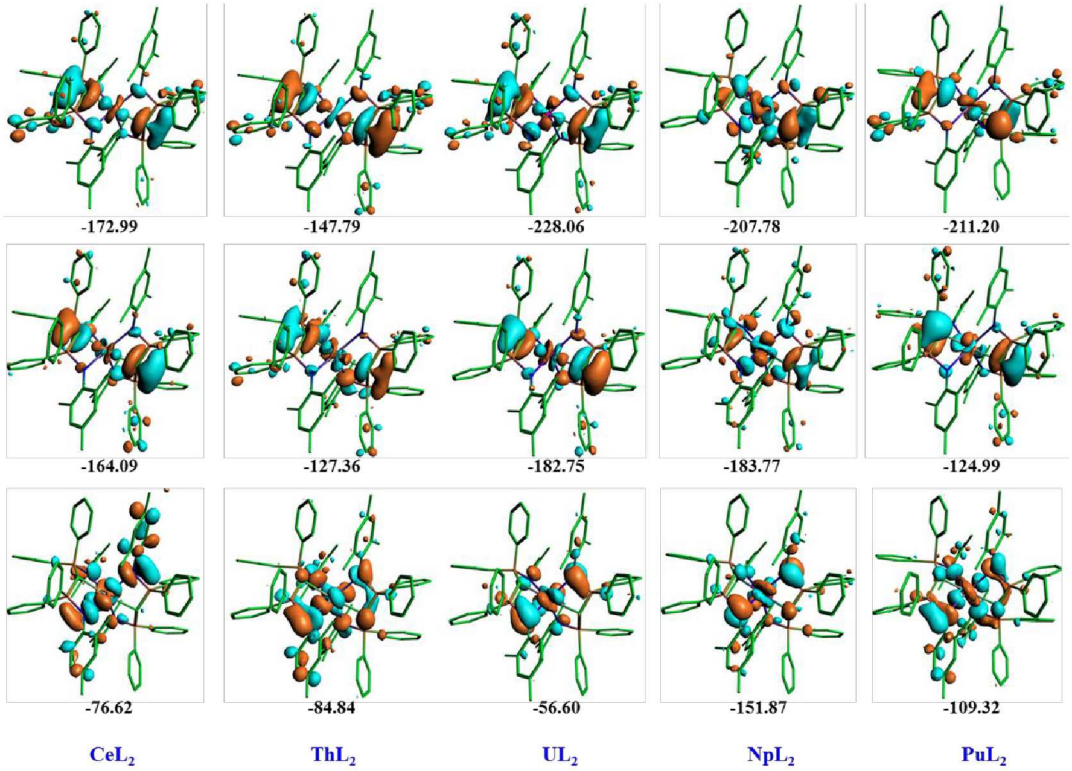

Fig. 5 Natural orbitals for the chemical valence (NOCV) with the largest contribution to the orbital interaction energy for the complexes ML_2. The corresponding orbital interaction energy contribution for each NOCV pair is indicated in kcal/mol.

Conclusions

Scalar-relativistic theory was employed to explore the nature of M-C bonds in lanthanide and actinide carbene complexes ML_2 (M=Ce, Th, U, Np and Pu). Based on the structural data available for UL_2 it was concluded that the geometrical parameters obtained with BP86 functional provides the best results among those considered. The five ML_2 possess similar structures with M-C multiple bonds, the Ce-C bond distances are close to the U-C distances, while the An-C bond distances decrease with increasing actinide atomic number, in parallel with decreasing An^{IV} ionic radii. A majority of the metal valence electrons occupy the (n-1)d and (n-2)f orbitals in the ML_2 (M=Ce, U, Np and Pu) complexes, whereas they reside predominantly in 6d orbitals for ThL_2. NBO analysis confirms that the M-C bonds are highly polarized with the valence electrons mainly localized on the carbon atoms. The M-C bonds exhibit double bond character with σ and π contributions, except for the Th-C bond with the π-only feature. There is similar composition and orbital contributions for Ce-C and U-C bonds, and the 6d orbital contribution to An-C bonds decreases while that of 5f orbitals increases across the

actinide series from Th to U to Pu. QTAIM analysis reveals that the M-C bonds in the complexes ML_2 have appreciable covalent characters, with the smallest covalency for the Th-C bonds. EST-NOCV analyses also indicate that the Th-C bonds exhibit the least covalency. The degree of covalency essentially depends on the contribution of f and d orbitals to the M-C bonds. A result of this dependence is that the Pu-C bonds are substantially covalent, while the Th-C bonds are less covalent. The results reveal that Ce-C and U-C bonding has remarkable similarity, and the covalency from Th-C to U-C to Pu-C gradually increases. Inclusion of Np and Pu in this work extends understanding to M-C bonding of later actinides.

Conflicts of interest

There are no conflicts to declare.

Acknowledgements

This work was supported by the National Natural Science Foundation of China (Grant Nos. 21477130, 21471152), the Major Program of National Natural Science Foundation of China (21790373) and the Science Challenge Project (TZ2016004). The results described in this work were obtained on the ScGrid of Supercomputing Center, Computer Network Information Center of Chinese Academy of Sciences. The work of J.K.G. was supported by the U.S. Department of Energy, Office of Basic Energy Sciences, Heavy Element Chemistry program at LBNL under Contract No. DE-AC02-05CH11231.

Notes and references

1 T. M. Trnka and R. H. Grubbs, *Acc. Chem. Res.*, 2001, **34**, 18-29.
2 G. C. Vougioukalakis and R. H. Grubbs, *Chem. Rev.*, 2010, **110**, 1746-1787.
3 Y. Xia, D. Qiu and J. Wang, *Chem. Rev.*, 2017, **117**, 13810-13889.
4 C.-M. Che, C.-M. Ho and J.-S. Huang, *Coord. Chem. Rev.*, 2007, **251**, 2145-2166.
5 J. Scott and D. J. Mindiola, *Dalton Trans.*, 2009, 8463-8472.
6 R. E. Cramer, R. B. Maynard, J. C. Paw and J. W. Gilje, *J. Am. Chem. Soc.*, 1981, **103**, 3589-3590.
7 K. Aparna, M. Ferguson and R. G. Cavell, *J. Am. Chem. Soc.*, 2000, **122**, 726-727.
8 T. Cantat, F. Jaroschik, F. Nief, L. Ricard, N. Mezailles and P. Le Floch, *Chem. Commun.*, 2005, 5178-5180.
9 T. Cantat, F. Jaroschik, L. Ricard, P. Le Floch, F. Nief and N. Mézailles, *Organometallics*, 2006, **25**, 1329-1332.
10 T. Cantat, T. Arliguie, A. Noël, P. Thuéry, M. Ephritikhine, P. L. Floch and N. Mézailles, *J. Am. Chem. Soc.*, 2009, **131**, 963-972.
11 O. J. Cooper, J. McMaster, W. Lewis, A. J. Blake and S. T. Liddle, *Dalton Trans.*, 2010, **39**, 5074-5076.
12 W. Ren, X. Deng, G. Zi and D.-C. Fang, *Dalton Trans.*, 2011, **40**, 9662-9664.
13 O. J. Cooper, D. P. Mills, J. McMaster, F. Moro, E. S. Davies, W. Lewis, A. J. Blake and S. T. Liddle, *Angew. Chem. Int. Ed.*, 2011, **50**, 2383-2386.
14 S. T. Liddle, D. P. Mills and A. J. Wooles, *Chem. Soc. Rev.*, 2011, **40**, 2164-2176.
15 J.-C. Tourneux, J.-C. Berthet, T. Cantat, P. Thuéry, N. Mézailles, P. Le Floch and M. Ephritikhine, *Organometallics*, 2011, **30**, 2957-2971.
16 D. P. Mills, O. J. Cooper, F. Tuna, E. J. McInnes, E. S. Davies, J. McMaster, F. Moro, W. Lewis, A. J. Blake and S. T. Liddle, *J. Am. Chem. Soc.*, 2012, **134**, 10047-10054.
17 M. Gregson, E. Lu, J. McMaster, W. Lewis, A. J. Blake and S. T. Liddle, *Angew. Chem. Int. Ed.*, 2013, **52**, 13016-13019.
18 O. J. Cooper, D. P. Mills, J. McMaster, F. Tuna, E. J. L. McInnes, W. Lewis, A. J. Blake and S. T. Liddle, *Chem.–Eur. J.*, 2013, **19**, 7071-7083.
19 M. Ephritikhine, *C. R. Chim.*, 2013, **16**, 391-405.
20 E. Lu, O. J. Cooper, J. McMaster, F. Tuna, E. J. L. McInnes, W. Lewis, A. J. Blake and S. T. Liddle, *Angew. Chem. Int. Ed.*, 2014, **53**, 6696-6700.
21 E. Lu, O. J. Cooper, F. Tuna, A. J. Wooles, N. Kaltsoyannis and S. T. Liddle, *Chem.–Eur. J.*, 2016, **22**, 11559-11563.
22 E. Lu, F. Tuna, W. Lewis, N. Kaltsoyannis and S. T. Liddle, *Chem.–Eur. J.*, 2016, **22**, 11554-11558.
23 M. Gregson, E. Lu, D. P. Mills, F. Tuna, E. J. L. McInnes, C. Hennig, A. C. Scheinost, J. McMaster, W. Lewis, A. J. Blake, A. Kerridge and S. T. Liddle, *Nat. Commun.*, 2017, **8**, 14137.
24 J. A. Seed, M. Gregson, F. Tuna, N. F. Chilton, A. J. Wooles, E. J. L. McInnes and S. T. Liddle, *Angew. Chem. Int. Ed.*, 2017, **56**, 11534-11538.
25 D. E. Smiles, G. Wu, P. Hrobárik and T. W. Hayton, *Organometallics*, 2017, **36**, 4519-4524.
26 S. Fortier, J. R. Walensky, G. Wu and T. W. Hayton, *J. Am. Chem. Soc.*, 2011, **133**, 6894-6897.
27 T. W. Hayton, *Chem. Commun.*, 2013, **49**, 2956-2973.
28 J. T. Lyon and L. Andrews, *Inorg. Chem.*, 2006, **45**, 1847-1852.
29 J. T. Lyon, H.-S. Hu, L. Andrews and J. Li, *Proc. Natl. Acad. Sci.*, 2007, **104**, 18919-18924.
30 H.-G. Cho and L. Andrews, *Coord. Chem. Rev.*, 2017, **335**, 76-102.
31 Q.-Y. Wu, J.-H. Lan, C.-Z. Wang, Y.-L. Zhao, Z.-F. Chai and W.-Q. Shi, *J. Phys. Chem. A*, 2015, **119**, 922-930.
32 M. B. Jones and A. J. Gaunt, *Chem. Rev.*, 2013, **113**, 1137-1198.
33 D. M. King and S. T. Liddle, *Coord. Chem. Rev.*, 2014, **266–267**, 2-15.
34 Z. Bao, H.-B. Zhao, N. Qu, G. Schreckenbach and Q.-J. Pan, *Dalton Trans.*, 2016, **45**, 15970-15982.
35 D.-M. Su, X.-J. Zheng, G. Schreckenbach and Q.-J. Pan, *Organometallics*, 2015, **34**, 5225-5232.
36 H.-S. Hu, Y.-H. Qiu, X.-G. Xiong, W. H. E. Schwarz and J. Li, *Chem. Sci.*, 2012, **3**, 2786.
37 M. Gregson, E. Lu, F. Tuna, E. J. L. McInnes, C. Hennig, A. C. Scheinost, J. McMaster, W. Lewis, A. J. Blake, A. Kerridge and S. T. Liddle, *Chem. Sci.*, 2016, **7**, 3286-3297.
38 A. Kerridge, *Chem. Commun.*, 2017, **53**, 6685-6695.

39 A. Yahia, L. Castro and L. Maron, *Chem.–Eur. J.*, 2010, **16**, 5564-5567.

40 M. J. Frisch, G. W. Trucks, H. B. Schlegel, G. E. Scuseria, M. A. Robb, J. R. Cheeseman, G. Scalmani, V. Barone, B. Mennucci, G. A. Petersson, H. Nakatsuji, M. Caricato, X. Li, H. P. Hratchian, A. F. Izmaylov, J. Bloino, G. Zheng, J. L. Sonnenberg, M. Hada, M. Ehara, K. Toyota, R. Fukuda, J. Hasegawa, M. Ishida, T. Nakajima, Y. Honda, O. Kitao, H. Nakai, T. Vreven, J. A. Montgomery Jr., J. E. Peralta, F. Ogliaro, M. J. Bearpark, J. Heyd, E. N. Brothers, K. N. Kudin, V. N. Staroverov, R. Kobayashi, J. Normand, K. Raghavachari, A. P. Rendell, J. C. Burant, S. S. Iyengar, J. Tomasi, M. Cossi, N. Rega, N. J. Millam, M. Klene, J. E. Knox, J. B. Cross, V. Bakken, C. Adamo, J. Jaramillo, R. Gomperts, R. E. Stratmann, O. Yazyev, A. J. Austin, R. Cammi, C. Pomelli, J. W. Ochterski, R. L. Martin, K. Morokuma, V. G. Zakrzewski, G. A. Voth, P. Salvador, J. J. Dannenberg, S. Dapprich, A. D. Daniels, Ö. Farkas, J. B. Foresman, J. V. Ortiz, J. Cioslowski and D. J. Fox, *Gaussian 09, Gaussian, Inc.: Wallingford, CT, USA, 2009*.

41 J. P. Perdew, *Phys. Rev. B*, 1986, **33**, 8822.

42 C. T. Lee, W. T. Yang and R. G. Parr, *Phys. Rev. B*, 1988, **37**, 785-789.

43 A. D. Becke, *J. Chem. Phys.*, 1993, **98**, 5648-5652.

44 Y. Zhao and D. Truhlar, *Theor. Chem. Acc.*, 2008, **120**, 215-241.

45 A. Klamt, *J. Phys. Chem.*, 1995, **99**, 2224-2235.

46 S. Sinnecker, A. Rajendran, A. Klamt, M. Diedenhofen and F. Neese, *J. Phys. Chem. A*, 2006, **110**, 2235-2245.

47 X. Cao, M. Dolg and H. Stoll, *J. Chem. Phys.*, 2003, **118**, 487-496.

48 X. Cao and M. Dolg, *J. Mol. Struct. (THEOCHEM)*, 2004, **673**, 203-209.

49 M. Dolg, H. Stoll and H. Preuss, *J. Chem. Phys.*, 1989, **90**, 1730-1734.

50 X. Y. Cao and M. Dolg, *J. Mol. Struct. (THEOCHEM)*, 2002, **581**, 139-147.

51 Q.-Y. Wu, J.-H. Lan, C.-Z. Wang, Y.-L. Zhao, Z.-F. Chai and W.-Q. Shi, *J. Phys. Chem. A*, 2014, **118**, 10273-10280.

52 Q.-Y. Wu, J.-H. Lan, C.-Z. Wang, Z.-P. Cheng, Z.-F. Chai, J. K. Gibson and W.-Q. Shi, *Dalton Trans.*, 2016, **45**, 3102-3110.

53 S. Ndambuki and T. Ziegler, *Inorg. Chem.*, 2013, **52**, 3860-3869.

54 G. te Velde, F. M. Bickelhaupt, E. J. Baerends, C. Fonseca Guerra, S. J. A. van Gisbergen, J. G. Snijders and T. Ziegler, *J. Comput. Chem.*, 2001, **22**, 931-967.

55 E. Van Lenthe and E. J. Baerends, *J. Comput. Chem.*, 2003, **24**, 1142-1156.

56 E. v. Lenthe, E. J. Baerends and J. G. Snijders, *J. Chem. Phys.*, 1993, **99**, 4597-4610.

57 R. F. W. Bader, *Atoms in Molecules: A Quantum Theory*, OUP: Oxford, U.K., 1990.

58 T. Lu and F. Chen, *J. Comput. Chem.*, 2012, **33**, 580-592.

59 V. Vetere, P. Maldivi and C. Adamo, *J. Comput. Chem.*, 2003, **24**, 850-858.

60 B. Averkiev, M. Mantina, R. Valero, I. Infante, A. Kovacs, D. Truhlar and L. Gagliardi, *Theor. Chem. Acc.*, 2011, **129**, 657-666.

61 Q.-Y. Wu, C.-Z. Wang, J.-H. Lan, C.-L. Xiao, X.-K. Wang, Y.-L. Zhao, Z.-F. Chai and W.-Q. Shi, *Inorg. Chem.*, 2014, **53**, 9607-9614.

62 R. G. Cavell, R. P. K. Babu and K. Aparna, *J. Organomet. Chem.*, 2001, **617**, 158-169.

63 R. D. Shannon, *Acta Cryst. A*, 1976, **32**, 751-767.

64 G. Ma, M. J. Ferguson, R. McDonald and R. G. Cavell, *Inorg. Chem.*, 2011, **50**, 6500-6508.

65 J. Su, C. J. Windorff, E. R. Batista, W. J. Evans, A. J. Gaunt, M. T. Janicke, S. A. Kozimor, B. L. Scott, D. H. Woen and P. Yang, *J. Am. Chem. Soc.*, 2018, **140**, 7425-7428.

66 I. Mayer, *Chem. Phys. Lett.*, 1983, **97**, 270-274.

67 P. L. Arnold, Z. R. Turner, N. Kaltsoyannis, P. Pelekanaki, R. M. Bellabarba and R. P. Tooze, *Chem.–Eur. J.*, 2010, **16**, 9623-9629.

68 B. Vlaisavljevich, P. Miró, C. J. Cramer, L. Gagliardi, I. Infante and S. T. Liddle, *Chem.–Eur. J.*, 2011, **17**, 8424-8433.

69 D. D. Schnaars, A. J. Gaunt, T. W. Hayton, M. B. Jones, I. Kirker, N. Kaltsoyannis, I. May, S. D. Reilly, B. L. Scott and G. Wu, *Inorg. Chem.*, 2012, **51**, 8557-8566.

70 N. Kaltsoyannis, *Inorg. Chem.*, 2013, **52**, 3407-3413.

71 J. Du and G. Jiang, *Inorg. Chem.*, 2017, **56**, 13794-13800.

72 M. J. Tassell and N. Kaltsoyannis, *Dalton Trans.*, 2010, **39**, 6719-6725.

73 I. Kirker and N. Kaltsoyannis, *Dalton Trans.*, 2011, **40**, 124-131.

74 M. L. Neidig, D. L. Clark and R. L. Martin, *Coord. Chem. Rev.*, 2013, **257**, 394-406.

75 D. Cremer and E. Kraka, *Angew. Chem. Int. Ed.*, 1984, **23**, 627-628.

76 A. D. Becke and K. E. Edgecombe, *J. Chem. Phys.*, 1990, **92**, 5397-5403.

77 B. Silvi and A. Savin, *Nature*, 1994, **371**, 683-686.

78 A. Savin, R. Nesper, S. Wengert and T. F. Fässler, *Angew. Chem. Int. Ed.*, 1997, **36**, 1808-1832.

Table of contents entry

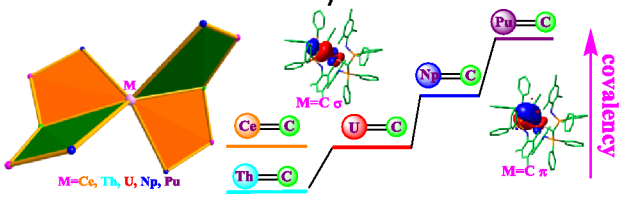

The An/Ln-C bonding nature was explored using relativistic theory. Inclusion of Np and Pu extends understanding to later actinides bonding.